Parametric analyses of pin-bone stresses in external fracture fixation devices

Journal of Orthopaedic Research
3:341–349, Raven Press, New York

Parametric Analyses of Pin-Bone Stresses in External Fracture Fixation Devices

R. Huiskes, *E. Y. S. Chao, and †T. E. Crippen

*Biomechanics Section, Laboratory for Experimental Orthopaedics, University of Nijmegen, Nijmegen, The Netherlands; *Orthopaedic Biomechanics Laboratory, Mayo Clinic, Mayo Foundation, Rochester, Minnesota; and †Department of Engineering Science, University of North Carolina, Charlotte, North Carolina, U.S.A.*

Summary: Problems occurring in the use of external fixators for bone fractures include pin-bone interface necrosis, infection, and loosening. These may be initiated and enhanced by pin-bone interface stress levels. Based on stress data from finite element method (FEM) models, an analytical "closed-form" model of the local pin-bone configuration in long-bone fracture fixation is developed. This model is relatively simple and useful for routine applications in combination with clinical studies and animal experiments. Although approximate, the most significant stress predictions in the pin-bone structure compare well with more sophisticated FEM analysis results.

The analytical model is used for extensive parametric analyses, investigating the effects on the pin-bone interface stress distribution of frame configuration parameters, pin diameter and modulus, bone dimensions, and elastic characteristics. The results indicate that these stresses may reach very high levels under unfavorable circumstances but can be drastically reduced by increasing the bending rigidity of the pin, reducing the side-bar separation and applying full-pin configuration in favor of half-pins. Key Words: External fixation—Biomechanics—Fracture healing.

External fixation of fractures in long bones has a long history of medical use, and the recent improvements in designs and materials have increased the popularity of these devices in orthopaedic surgery and traumatology. Many configurations are available, which can be classified as unilateral (half frames), bilateral (full frames), triangular, and quadrilateral (2).

Because external fixators are load-carrying devices, a certain amount of load must be transferred from each transcortical pin to the surrounding bone. The local pin-bone stresses, which reach high levels during weight-bearing in the presence of a fracture gap, could cause pressure necrosis and subsequent infection and loosening (7,14). The pin-bone stress levels and their dependence on bone and frame characteristics are the subject of this paper.

Previous work on external fixators includes studies of various biomechanical aspects (1–5,9,13). Pin-bone interface stresses were investigated by Chao and An (4), Harris et al. (9), and Manley et al. (13). Since pin-bone interface stresses cannot be measured directly, their levels and patterns must be estimated from experimental or analytical models. An experimental study was reported by Manley et al. (13) to investigate the stress distribution in a plate around a loaded pin. Using photoelastic material, they modeled the cortex as a two-dimensional plate with metal pins of 4, 5, 6, and 7 mm diameters inserted in holes and visualized the stress fringes in the plate, around the pins,

Address correspondence and reprint requests to Dr. R. Huiskes at Biomechanics Section, Laboratory for Experimental Orthopaedics, University of Nijmegen, 6500 HB Nijmegen, The Netherlands.

The results of this study were presented in parts at the biomechanics symposium, American Society of Mechanical Engineers, Boulder, Colorado, June 1981, and at the 29th annual meeting of the Orthopaedic Research Society, Anaheim, California, March 8–10, 1983.

under polarized light. A local compressive stress distribution was evident at the pin-plate interface, steeply fading away from the hole. The stress levels were lower for the thicker pins. Coating of the pins with plastic materials tended to reduce the stress levels in the plate as well. An analytical study, which is discussed later in this paper, was carried out by Harris et al. (9). A three-dimensional (3D) finite element method (FEM) analysis of the local pin-bone configuration was reported by Chao and An (4). This analysis provided data on the local stress patterns and peak-stress levels in the bone around the pin, but it has not been subject to parametric analysis. The FEM has a high potential for accuracy and validity in predicting stresses in geometrically complex structures and thus is an attractive tool for stress evaluations in orthopaedic structures (12). However, in some cases it is possible to develop a model based on traditional theories of solid mechanics ("closed-form" theories). These models yield their results in readily interpretable formulas, rather than in numerical form such as in FEM models and are thus most suitable for extensive parametric analysis. Using FEM results as a database, a model of this kind with respect to the pin-bone load transfer is described and applied in this paper to estimate the pin-bone stress levels and to establish the effectiveness of measures possible for stress reductions.

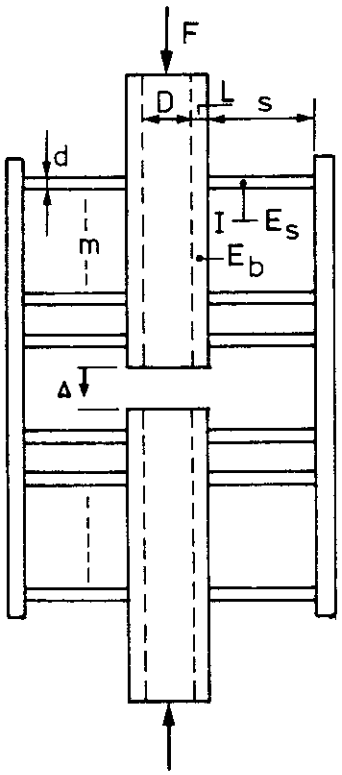

FIG. 1. Schematic outline of an external fixation frame configuration, indicating the most significant parameters, further defined in Table 1.

METHODS

FEM Models

A schematic illustration of the EFF configuration (bilateral frame and full pin) is shown in Fig. 1. The symbols depicting the parameters of interest are defined in Table 1.

The 3D FEM model reported earlier (4) assumed a bilateral frame configuration as well and its parameter values were as shown under "reference values" in Table 1. The local pin load was determined based on an analysis of the entire fixation structure (5). This 3D FEM model represented a part of the bone and one pin only, assuming that the pin-bone stress concentrations are local phenomena. That this assumption is warranted was supported by the results of the analysis. At a distance of approximately 10 mm from the pin the local stress concentrations were reduced to the levels of the nominal bone stress. The same phenomenon was evident in the results of the photoelastic analysis of Manley et al. (13). The local character of the pin-bone stress transfer also forms the basis of the newly developed model discussed here.

Because the pin radius is much smaller than the bone "radius" and the most significant stresses in the bone occur in a longitudinal plane, it is attractive to model the cortices on both sides as flat plates. In this case an axisymmetric FEM model can be developed, with the pin axis as the axis of

TABLE 1. *Reference values of the parameters illustrated in Fig. 1*

Parameter	Symbol	Unit	Reference value
Axial bone force	F	N	445
Intramedullary width	D	mm	16
Cortical thickness	L	mm	4.8
Side-bar separation	s	mm	63.5
Number of pins/fracture side	m	—	3
Young's modulus bone	E_b	MPa	1.52×10^4
Young's modulus pin	E_s	MPa	2.00×10^5
Pin diameter	d	mm	3.96
Pin area moment	I	mm^4	12.1
Fracture deformation	Δ	mm	Variable

symmetry (Fig. 2). For the bilateral frame, full-pin configuration in axial bone loading, the structure is also symmetric with respect to the middiaphyseal plane, and thus only one cortex has to be taken into account if the appropriate boundary conditions are applied.

Whereas the pin-bone connection in the 3D FEM model was assumed to be rigidly bonded at the interface, the axisymmetric FEM model assumes either fully bonded or sliding interfaces. In the latter case no shear stresses are transferred, but tensile stresses do occur in addition to compressive stresses. In the axisymmetric model all stresses are expressed as sine or cosine functions of the tangential coordinate ϕ. The axial (bending) stress in the pin, for example, can be denoted as:

$$\sigma_z = \hat{\sigma}_z \cos \phi \qquad (1)$$

where $\hat{\sigma}_z$, the stress "amplitude," is a function of r and z only. The pin-bone interface radial (transverse) stress σ_r and the tangential shear stress $\tau_{r\phi}$ can be expressed accordingly as:

$$\sigma_r = \hat{\sigma}_r \cos \phi \text{ and } \tau_{r\phi} = \hat{\tau}_r \sin \phi \qquad (2)$$

This stress distribution in a cross section at the pin-bone interface is illustrated in Fig. 3 (left). These stress patterns, obvious in the axisymmetric model, were also found in the 3D FEM model. Figure 4 shows a comparison of radial (transverse)

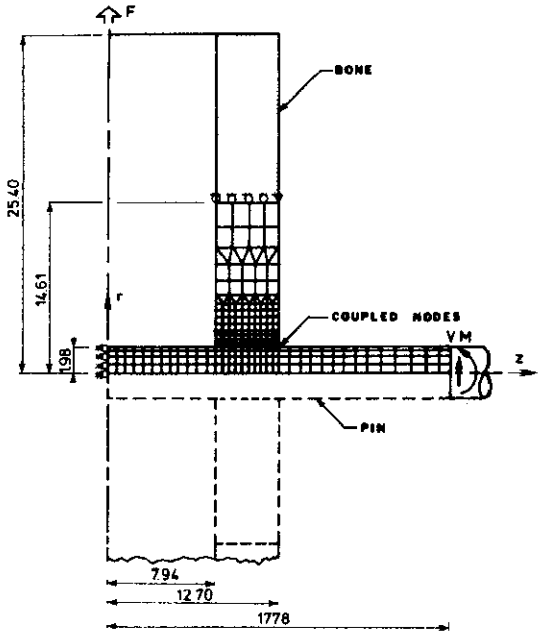

FIG. 2. Axisymmetric finite element method model of the local pin-bone configuration.

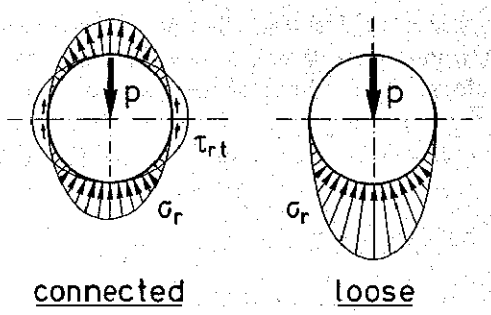

FIG. 3. Illustration of the pin-bone interface stress distributions in a section through the pin in the case of a rigidly bonded (connected) interface (left) and a loose interface (right).

stress amplitudes ($\hat{\sigma}_r$) along the (superior) pin-bone connection as calculated in the axisymmetric model (both for bonded and sliding interfaces), and as calculated in the 3D FEM model. Compressive stress is found in the outer part of the cortex and tensile stress in the inner part; on the other (inferior) side of the pin these trends are reversed.

If tensile stresses cannot be transferred at the pin-bone connection, which is a more realistic assumption, only half the interface in a cross section is under (compressive) stress, as illustrated in Fig. 3 (right).

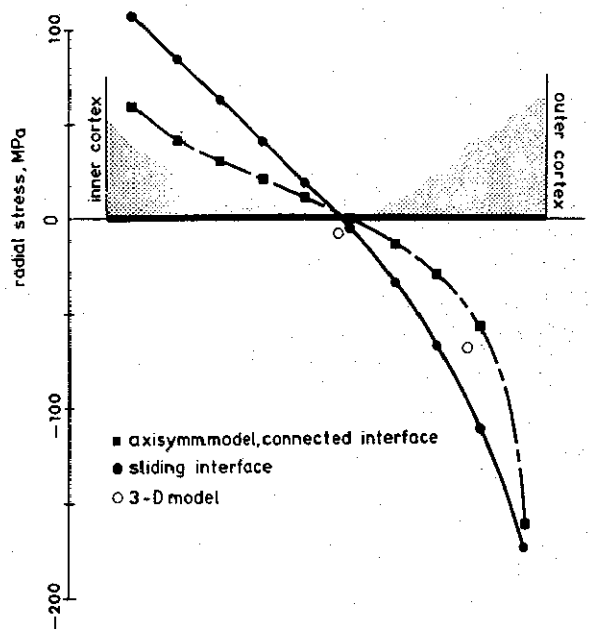

FIG. 4. A comparison of radial direct stresses, perpendicular to the pin-bone interface, in the bone cortex, shows results of the axisymmetric finite element method (FEM) model (bonded or connected and sliding interface) and the three-dimensional (3D) FEM model (bonded interface).

As in (11) we define the lumped transverse load $p(z)$ (N/mm) transferred in a local cross section from the pin to the bone at the pin surface as:

$$p(z) = \frac{d}{2}\int_0^{2\pi}(\sigma_r \cos\phi - \tau_{r\phi}\sin\phi)\, d\,\phi \quad (3)$$

For a bonded pin (Fig. 3) this gives:

$$p(z) = \frac{\pi}{2}\, d(\hat{\sigma}_r - \hat{\tau}_{r\phi}) \quad (4)$$

If no shear stress is transferred (sliding pin), this reduces to $p(z) = \pi/2\ d\ \hat{\sigma}_r$. For an unbonded pin (no shear and no tensile stress) the transverse stress is transferred across half the interface, hence:

$$p(z) = \frac{\pi}{4}\, d\ \hat{\sigma}_r \quad (5)$$

Equation 4 is used to relate the results of the axisymmetric FEM model to those of the analytical model, for which the lumped transverse load p is a principal variable. Equation 5 is used to transform values for p, calculated with that model, into actual stresses for the case that tensile loosening can occur at the pin-bone interface.

Analytical Model

The analytical (closed-form) model of the local pin-bone configuration is derived from the above FEM models using the assumptions of beam-on-elastic-foundation (BEF) theory (10,11). We assume that the pin behaves in accordance with linear elastic beam theory, whereas the surrounding bone acts as a linear elastic foundation of continuous spring-like elements (Winkler hypothesis, Fig. 5).

Owing to the assumptions used, a relation exists between the lumped transverse load $p(x)$ transferred from the pin to the bone at the interface in a cross section[1] and the local deflection of the pin $u(x)$:

$$p = -E_s I\, \frac{d^4u}{dx^4} \quad (6)$$

$$p = ku \quad (7)$$

where k (N/mm^2) is the foundation modulus.

Combining Eqs. 6 and 7 gives a differential equation in $u(x)$ for the regions $x = x_1$, $x = x_2$, and $x = x_3$ that can be solved analytically. The solution for

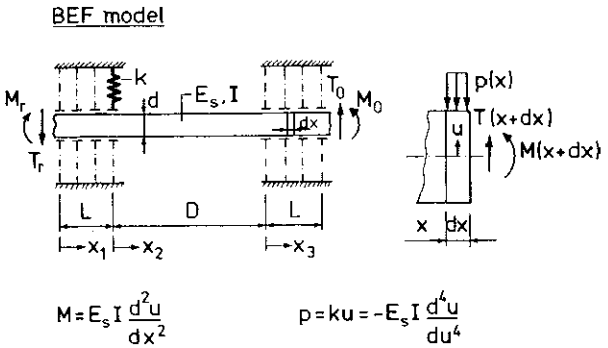

FIG. 5. Definition of the beam-on-elastic-foundation (BEF) model of the local pin-bone configuration.

$u(x)$ also gives the lumped transverse load $p(x)$, the internal pin bending moment $M(x)$, and the transverse force $T(x)$. The appropriate boundary conditions at $x_1 = 0$, $x_1 = L$, $x_2 = 0$, $x_2 = D$, $x_3 = 0$, and $x_3 = L$ give the integration constants for each region. The solution is presented in Appendix A.

The values for the external loads in the pin (M_0, T_0, M_r, and T_r, Fig. 5) are taken from FEM beam-analyses of whole frame configurations (5), as in the FEM models discussed previously. The model can represent bilateral (full-pin) configurations ($M_r = M_0$, $T_r = -T_0$), comparable with the FEM models, but also unilateral (half-pin) configurations ($M_r = T_r = 0$). In fact, it can be applied for arbitrary situations as long as the external loads are known.

No attempt was made to determine the foundation modulus directly. Owing to its definition ($k = p/u$), k is not directly dependent on the pin diameter and, because we assume a linear system, k must be proportional to the bone Young's modulus (11). Hence, $k = \alpha E_b$.

The value of α is assumed constant over the width of the cortex and is assessed by fitting the analytical results to those of the axisymmetric FEM model. The comparison, for $\alpha = 5.8$, is shown in Fig. 6 with respect to the lumped transverse load

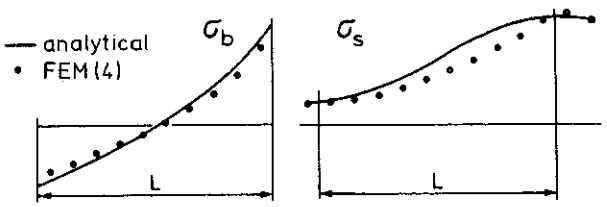

FIG. 6. A comparison of pin-bone stresses in the bone cortex calculated with the axisymmetric finite element method (FEM) model (sliding interface) and the analytical beam-on-elastic-foundation model, concerning pin-bone interface stress (left) and pin bending stress (right).

[1] Note that in the analytical model the pin axis is denoted as the x-axis, whereas in the axisymmetric FEM model it is denoted as the z-axis.

$p(x)$ at the pin-bone interface and the pin bending moment $M(x)$. A parametric analysis with respect to α showed that the courses of these curves are not very sensitive to its value; varying α between 4 and 8 gave less than 10% change in the peak values of $p(x)$, for example. The value of α was kept at 5.8 throughout the following parametric analysis.

RESULTS

Frame Configuration

Pin (bending) stresses and pin-bone interface stresses in the bilateral (full-pin) and unilateral (half-pin) frame configurations are shown in Fig. 7. The interface stresses are average values $[p(x)/d]$ in a cross section, and thus the actual peak values will be a factor $4/\pi$ higher (Eq. 5). The external loads M_0 and T_0 were taken from full-frame analyses (5), M_0 = 2,360 Nmm and T_0 = 74 N in the full-pin, and M_0 = 4,709 Nmm and T_0 = 148 N in the half-pin. The other parameter values are as in the reference case (Table 1).

In both cases the maximal pin stresses occur just outside the cortex; the stress patterns of the parts within the bone seem to be of little further interest. The pin-bone interface peak stresses are approximately 100% higher in the unilateral, half-pin configuration. Although the contralateral cortex is not very heavily stressed in this case, its support is very important. If eliminated, the peak interface stress values increase by more than 30%.

In the case of a triangular frame the peak interface stresses are reduced by approximately 30% compared with the bilateral one. In a quadrilateral frame they drop by approximately 50%.

External Loads and Side-Bar Separation

The interface stress patterns in Fig. 7 already indicate that the external bending moment M_0 contributes more than the transverse force T_0. In both of the configurations T_0 in fact contributes only approximately 8% of the peak stress. This opens interesting possibilities for stress reductions. The transverse force T_0 is absolutely necessary for the load-carrying capacity of the external fixation device, since it balances the axial load. However, the bending moment M_0 is only introduced through the flexibility of the system, hence it may be minimized.

It was found in full-frame FEM models (5) that for a well-fixed pin, clamped on both sides:

$$M_0 \approx \frac{s}{2} T_0 \qquad (8)$$

in both the full-pin and the half-pin configurations. Hence, M_0 can be minimized by minimizing s, the side-bar separation.

Because M_0 contributes almost 92% of the pin-

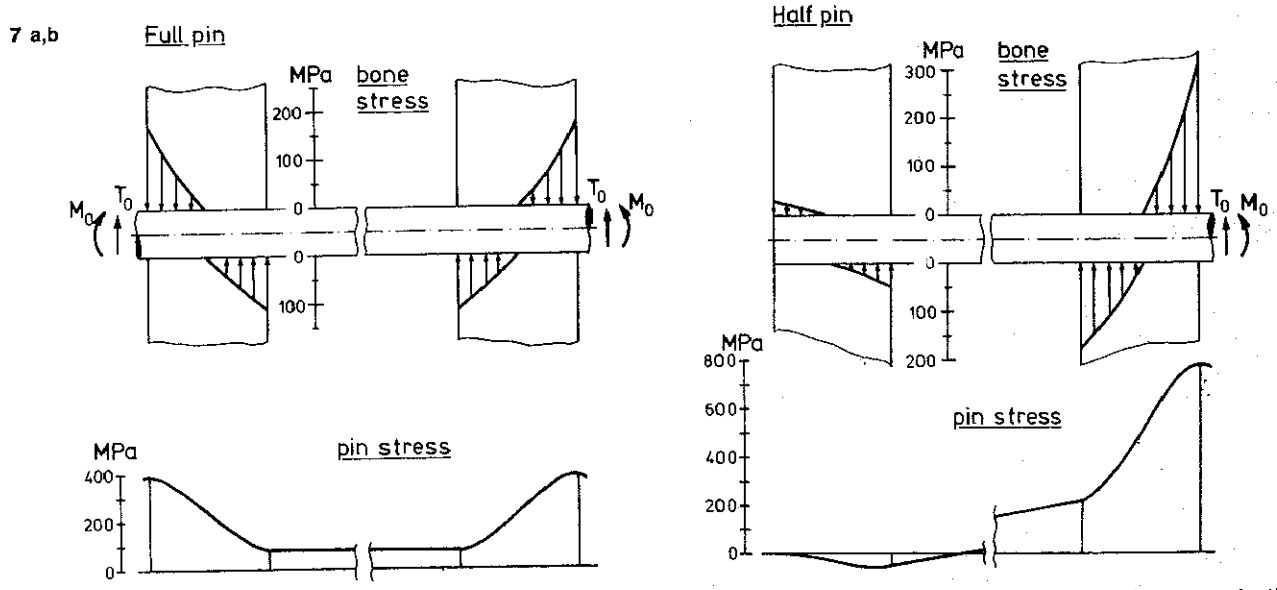

FIG. 7. Pin-bone interface stresses and pin bending stresses along the pin length, as calculated with the beam-on-elastic-foundation model, for a full-pin (bilateral) configuration **(a)** and a half-pin (unilateral) configuration **(b)** (gap at the fracture site; all other parameters as in Table 1).

bone interface stresses, Eq. 8 indicates that the peak stress values vary almost linearly with the side-bar separation, as confirmed in calculations with varying s (Fig. 8).

Pin Materials and Thickness

Titanium pins result in approximately 20 to 25% higher peak stresses at the pin-bone interface as compared with stainless-steel pins (Fig. 9). This is caused by the higher flexibility of titanium. The pin flexibility is even more affected by the pin diameter, a reduction of which increases the pine-bone interface stresses (and the pin-bending stresses) progressively (Fig. 10). This effect is caused by two phenomena: (a) the increase of pin flexibility (a fourth-power relation) and (b) the decrease of the bearing surface for the transverse load (a linear relation).

Other Parameters

The effects of the other model parameters on the pin-bone interface stresses are not very extensive. Influences of variations of the bone modulus (E_b), the medullary canal width (D), and the cortical thickness (L) over a reasonable range are shown in Fig. 11. All other parameters here were taken according to the reference case (Table 1).

DISCUSSION

Because of its simplicity, the BEF model is an attractive alternative to FEM models, in particular for rapid stress evaluations and extensive parametric analyses. Compared with the more sophisticated FEM models, it can only supply data on pin stresses and on transverse pin-bone interface stresses. Of course, these are the primary expedi-

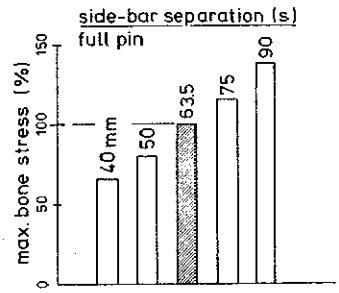

FIG. 8. Effect of the side-bar separation (s) on the peak bone stress at the pin-bone interface, relative to the reference configuration.

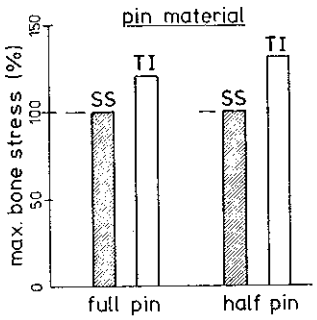

FIG. 9. Effect of the pin modulus (stainless steel versus titanium alloy) on the peak bone stress at the pin-bone interface.

ents of load transfer and therefore the most important. It must be remembered, however, that the BEF model is a rough approximate one, and although the results compare well with those of the FEM models, these too are simplified representations of the real structure. Variations in bone properties (nonhomogeneities) and local irregularities in the pin-bone interface, not accounted for, will affect the stress patterns. Uncertain issues are the actual stress values at the outer points of the cortices at the pin-bone interface, which are highly susceptible to the actual, local geometries. These are not described in detail by the FEM models nor by the BEF model. In accordance with the results obtained in comparable structures (e.g., 8) it is assumed that, although the actual stress values in these outer (singular) points are uncertain, the stresses in the immediate neighborhood are described reasonably well. Therefore, the peak stress values discussed here should be regarded as representing the load transferred in the outer regions, rather than the actual stresses in the outer points.

A weak point of the simple BEF theory is the

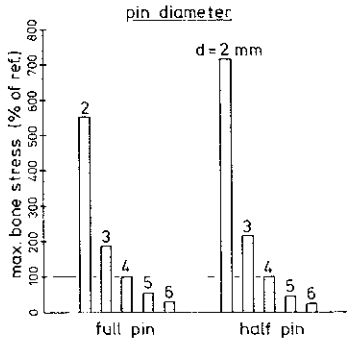

FIG. 10. Effect of the pin diameter on the peak bone stress at the pin-bone interface, relative to the reference configuration.

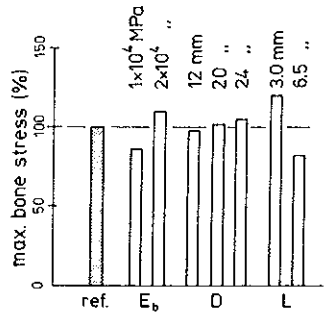

FIG. 11. Effects of changes in the bone modulus (E_b), the intramedullary width (D), and the cortical thickness (L) on the peak bone stress at the pin-bone interface, relative to the reference configuration.

assumption of the Winkler hypothesis. Although it was shown repeatedly that this hypothesis is approximately fulfilled in continuous foundations (e.g., 6), it is certain that the foundation modulus is in reality not uniform over the pin foundation length. Using additional FEM analysis with refined meshes, it was found that the foundation modulus is reduced approximately 17% at the edges but is practically homogeneous over 90% of the foundation length. So again, the Winkler assumption mainly affects the actual stress values at the outer points and has little effect on the overall stress distribution along the pin length.

It is possible to take the above effects into account in a more sophisticated analytical model (e.g., 6). However, in view of the biological complexities, it is questionable whether significant gains could be made in terms of precise predictions of actual stress values. From the viewpoint of suitability for rapid, approximate stress evaluations and extensive parametric analysis, on the other hand, such a complicated model would certainly be less attractive.

Conversely, it is possible to simplify the model further. Harris et al. (9) proposed a very simple model based on overall equilibrium. However, the peak pin-bone interface stresses reported by these authors are on the order of 10 times lower than found here. This discrepancy is due to the fact that Harris et al. (9) assumed the transverse stresses along the pin-bone interface to be uniform. In doing so, the pin flexibility is neglected, and the bending moment in the pin, which contributes up to 92% of the peak bone stresses, is not accounted for. A better way of simplifying the model further is to assume the transverse stress distribution along the pin-bone interface to be linear (Fig. 12). In this case the equations in the BEF model are simplified further (Appendix B), and the peak pin-bone interface compressive stress in a full-pin configuration can be roughly approximated by:

$$\bar{\sigma}_{b\,\max} \approx T_0 s / \left[d \left(\frac{8E_s I}{LDk} + \frac{L^2}{3} \right) \right] \qquad (9)$$

The deviation in the predictions of this linear model are less than 25% when compared with the BEF model, always on the lower side, as long as the pins are not too flexible ($d \geq 3$ mm). In this formula the effect of the pin bending moment is accounted for via Eq. 8. Although this linear model is even less precise than the BEF model, it describes the parametric effects discussed earlier just as well, provided these are interpreted in a relative sense.

Finally, where the BEF model itself is concerned, it must be stressed once more that the results discussed here refer to smooth, unthreaded pins. In the case of threaded pins, shearing loads will be transferred to the bone at the pin-bone interface, in addition to transverse loads. Consequently, in view of equilibrium considerations the latter will on the average be reduced somewhat (Fig. 4, connected versus sliding interface).

The results obtained here with the various models suggest that peak pin-bone interface stresses on the order of 300 MPa are well feasible (e.g., Fig. 7b). This represents a worst-case situation in the sense that a complete fracture gap is assumed. The axial load, however, is only approximately 75% of body weight. Assuming a 3 times body weight force and partial bone healing to the extent that only 5% of the load is transferred through the external fixator (1), the result, in this case, would be a peak pin-bone stress of 60 MPa. It is obvious from the previous discussion that these absolute stress values must be regarded with caution in view of the many

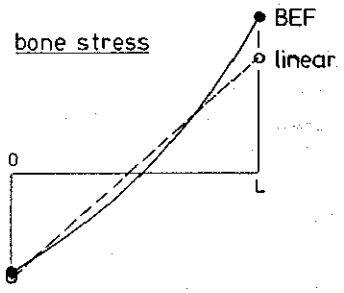

FIG. 12. If the pin-bone interface stresses in the cortex are assumed linear along the pin, the beam-on-elastic-foundation (BEF) formulas are simplified in such a manner that a relatively simple formula for the peak stress evolves (Appendix B).

assumptions underlying the models. It merely suggests that the peak pin-bone stress values are potentially of significant magnitude when compared with yield strength values reported for cortical bone.

Regarding the parametric effects, which are emphasized in this paper, it is found that effective precautions can be taken to reduce the stresses considerably, thereby reducing the chances for local bone yielding, necrosis, and loosening. These precautions include increasing the pin diameter and the Young's modulus of the pin material and reducing the side-bar separation. In addition, the use of full-pin configurations has considerable advantages over half-pin configurations where the pin stresses and pin-bone stresses are concerned. Evidently, all measures taken to decrease the stresses increase the frame rigidity at the same time.

APPENDIX A

BEF Model

Referring to Fig. 5 in the main text, we have the following relations between the pin internal loads $M(x)$, $T(x)$, and $p(x)$ and the pin deflection $u(x)$ in accordance with linear elastic beam theory

$$M(x) = E_s I u'' \tag{A1}$$

$$T(x) = -E_s I u''' \tag{A2}$$

$$p(x) = -E_s I u'''' \tag{A3}$$

where u'' is the second derivative of $u(x)$ with respect to x, and so on. In addition the beam deflection angle $\phi(x)$ can be expressed as

$$\phi(x) = u' \tag{A4}$$

while the BEF theory assumes that

$$p = ku \tag{A5}$$

in the regions $x = x_1$ and $x = x_3$, where k is the foundation modulus.

Combining Eqs. A3 and A5 in the regions $x = x_1$ and $x = x_3$ gives

$$u_i'''' + \frac{k}{E_s I} u_i = 0, \; i = 1,3 \tag{A6}$$

with the solution

$$u_i(x_i) = \underline{a}_i^T \underline{f}(x_i), \; i = 1,3 \tag{A7}$$

where:

$$\underline{a}_i^T = (a_{i1}, a_{i2}, a_{i3}, a_{i4})$$

$$\underline{f}^T(x_i) = (e^{\lambda x_i} \cos \lambda x_i, e^{\lambda x_i} \sin \lambda x_i, e^{-\lambda x_i} \cos \lambda x_i, e^{-\lambda x_i} \sin \lambda x_i)$$

$$\lambda = (k/4E_s I)^{\frac{1}{4}}$$

The eight integration constants $\underline{a}_i^T$ $(i = 1,3)$ are evaluated with the boundary conditions

at $x_1 = 0$: $u_1''(0) = M_r/E_s I$ and $u_1'''(0) = -T_r/E_s I$

at $x_3 = L$: $u_3''(L) = M_0/E_s I$ and $u_3'''(L) = -T_0/E_s I$

at $x_1 = L$ and $x_3 = 0$:

$$u_3''(0) - u_1''(L) - Du_3'''(0) = 0$$

$$u_3'''(0) - u_1'''(L) = 0$$

$$u_3'(0) - u_1'(L) - Du_3''(0) + \frac{D^2}{2} u_3'''(0) = 0$$

$$u_3(0) - u_1(L) - Du_1'(L) - \frac{D^2}{2} u_3'' + \frac{D^3}{3} u_3''' = 0$$

APPENDIX B

Linear BEF Model (Full-Pin)

Referring again to Fig. 5 of the main text, we define (in the region $x = x_2$) $M(D/2) = M_m$, $T(D/2) = T_m$, $u(D/2) = u_m$, and $\phi(D/2) = u'(D/2) = \phi_m$. In view of considerations of symmetry we have $T_m = \phi_m = 0$. Considering equilibrium yields

$$M_m - M_0 - \int_0^L p(x_3)(L - x_3)dx_3 = 0 \tag{B1}$$

$$T_0 - \int_0^L p(x_3)dx_3 = 0 \tag{B2}$$

Symmetry in the pin deflections gives

$$\phi_m = \phi(x_3 = 0) - \frac{D}{2E_s I} M_m = 0 \tag{B3}$$

Using $p = ku$, hence $\phi = u' = p'/k$ transforms (B3) into

$$p'(x_3 = 0) - \frac{Dk}{2E_s I} M_m = 0 \tag{B4}$$

The specific assumption in this case is that $p(x_3)$ is linear in x_3,

$$p(x_3) = c_1 x_3 + c_2 \tag{B5}$$

Hence, Eqs. B1, B2, and B4 contain three unknowns (c_1, c_2, and M_m) and can be solved. Using $M_0 \approx s/2\ T_0$ (Eq. 8 in the main text) and $\bar{\sigma}_{b\,\max} \approx p(x_3 = L)/d$ we find

$$\bar{\sigma}_{b\,\max} \approx \frac{T_0}{dL}\left[1 + L^2(L + s)/\left(\frac{8E_sI}{Dk} + \frac{L^3}{3}\right)\right] \quad \text{(B6)}$$

Since $8E_sI/LDk \ll L^2 \ll Ls$, if the pins are not too thin (d $\geqslant$ 3 mm), this can be simplified to

$$\bar{\sigma}_{b\,\max} \approx T_0 s/\left[d\left(\frac{8E_sI}{LDk} + \frac{L^2}{3}\right)\right] \quad \text{(B7)}$$

Acknowledgment: During the execution of this work the principal author was a guest of the Biomechanics Laboratory, Mayo Clinic/Mayo Foundation, and partly supported by Grant No. 95/118 from the Netherlands Organisation for the Advancement of Pure Research (ZWO).

REFERENCES

1. Beaupre GS, Hayes WC, Jofe MH, White AA: Monitoring fracture site properties with external fixation. *J Biomech Eng* 105:120–126, 1983
2. Behrens F: External skeletal fixation. *Instr Course Lect* 30:112–184, 1981
3. Briggs BT, Chao EYS: The mechanical performance of the standard Hoffmann-Vidal external fixation apparatus. *J Bone Joint Surg [Am]* 64:566–573, 1982
4. Chao EYS, An KN: Biomechanical analysis of external fixation devices for the treatment of open bone fracture. In: *Finite Elements in Biomechanics,* ed by RH Gallagher, BR Simon, PC Johnson, JF Gross. New York, John Wiley and Sons, 1982
5. Chao EYS, Kasman RA, An KN: Rigidity and stress analysis of external fracture fixation devices—A theoretical approach. *J Biomech* 15:971–983, 1982
6. Gallagher AP: Bending of a free beam on an elastic foundation. *J Appl Mech* 50:463–465, 1983
7. Green SA: Pin tract infection. In: *Complications of External Skeletal Fixation.* Springfield, Illinois, CC Thomas, 1981
8. Haritos GK, Keer LM: Stress analysis for an elastic half space containing an embedded rigid block. *Int J Solids Structures* 16:19–40, 1980
9. Harris JD, Evans M, Kenwright J: Safe stress levels at the screw interface of an external fixator for long bone fractures. In: *Mechanical Factors and the Skeleton,* ed by I Stokes, London, John Libbey, 1981
10. Hetényi M: *Beams on Elastic Foundation.* Ann Arbor, Michigan, University of Michigan Press, 1946
11. Huiskes R: Some fundamental aspects of human joint replacement. *Acta Orthop Scand* [Suppl] 185:100–209, 1980
12. Huiskes R, Chao EYS: A survey of finite element methods in orthopaedic biomechanics: The first decade. *J Biomech* 16:385–410, 1983
13. Manley MT, Hurst L, Hindes R, Dee R, Chiang FP: Effects of low-modulus coatings on pin-bone contact stresses in external fixation. *J Orthop Res* 2:385–392, 1984
14. Schatzker J, Horne JG, Sumner-Smith G: The effects of movement on the holding power of screws in bone. *Clin Orthop* 111:257–262, 1975